Proceedings World Geothermal Congress 2020+1
Reykjavik, Iceland, April - October 2021

Geothermal power plants with improved environmental performance: assessment of the potential for an Italian site

Daniele Fiaschi[a], Martina Leveni[b], Giampaolo Manfrida[c], Barbara Mendecka[d], Lorenzo Talluri[e] and Claudio Zuffi[f]

[a] University of Florence, Florence, Italy, daniele.fiaschi@unifi.it
[b] The Ohio State University, Columbus, Ohio, leveni.1@osu.edu
[c] University of Florence, Florence, Italy, giampaolo.manfrida@unifi.it
[d] CSGI, Florence, Italy, barbara.mendecka@unifi.it
[e] University of Florence, Florence, Italy, lorenzo.talluri@unifi.it
[f] CSGI, Florence, Italy, zuffi@csgi.unifi.it

Keywords: Geothermal energy; Organic Rankine Cycle; Non-Condensable Gases; Sustainable Development.

ABSTRACT

The goal of a 2050 Carbon neutral scenario is providing a big push for the development of renewable energy technology. Amongst renewables, geothermal energy could become a considerable contributor to the reduction of greenhouse emissions, thanks to the new technologies that have been developed in the last years. One of the most interesting new technologies is the total reinjection one, which guarantees the total reinjection of the geothermal fluid (including Non-Condensable Gases – NCGs, which are currently vented to the atmosphere with the "traditional" technologies).

Within this manuscript, a solution for complete NCGs reinjection is presented, and the Torre Alfina geothermal case study is analysed. The Torre Alfina geothermal site is a water-dominated reservoir at relatively high pressure (44 bar) and a temperature of 140°C, with moderate content of Non Condensable Gases (2%).

The developed power plant models include energy and exergy balances, as well as exergo-economic and exergo-environmental analysis. The overall environmental performance is evaluated by Environmental Footprint 2.0 methodology. Different solutions are compared, considering the possibility of sub- or super-critical power cycles as well as different renewables. For the subcritical case, the obtained LCOE is 13.33 c€/kWh, while for the supercritical cycle the obtained LCOE is 13.11 c€/kWh. The developed LCA confirms that geothermal power plants with complete NCG reinjection are among the cleanest renewable energy technologies

1. INTRODUCTION

Geothermal energy has great potential for development in many European countries. However, the advantages of its use for electricity production and for heating and cooling are not widely known. Recently, geothermal energy production in some regions, faces a negative perception, especially in terms of environmental performance, which could seriously hamper its market uptake. Therefore, environmental impact assessment is a fundamental prerequisite for the exploitation of deep geothermal resources. The concept of Life Cycle Assessment (LCA) allows to analyse and compare the environmental impacts (consumption of primary resources, emissions, induced modifications of ecosystems, damage to health, etc.) of different energy production technologies during their life cycle phases, with a cradle-to-grave approach: from raw material extraction to production, transport, use, and end-of-life.

One of the aspects that need to be analysed in detail from an environmental point of view is the release to the atmosphere of the Non-Condensable Gases (NCGs). NCGs are mainly composed of CO_2, but also other contaminants are present, such as CH_4, H_2S, Hg and Heavy metals (Kagel et al., 2005; Rice et al., 2014). The traditional geothermal power plants utilized abatement technology in order to reduce the contaminants, for example in Italy, a chemical scrubbing and chemical scrubbing and adsorption - AMIS ® (Baldacci et al., 2005), effectively removing H_2S, Hg, and NH_3. Nonetheless, greenhouse emissions continue to be an unsolved issue with the current technology, with an average documented value of 122 mg/kWh but with a relatively wide range of values as testified by (Bruscoli et al., 2015; Eberle et al., 2017).

The reasons above have led several researchers to explore several environmental-friendly geothermal solutions. One of the most promising is the total reinjection configuration, which allows for the preservation of the reservoir, as well as to avoid any kind of emission. Some of the proposed solutions evaluate a two-phase reinjection (Shafaei et al., 2012) or CO_2 mineralization in the reservoir (Snæbjörnsdóttir et al., 2017). These solutions leverage from the experience in the Oil&Gas (Guo et al., 2017) and Carbon Capture and Storage (CCS) fields.

2. MODELS FOR THE SOLUBILITY OF NCGs IN THE BRINE

Most solutions for NCGs reinjection or disposal must face matters related with solubility of NCGs in the brine. NCGs are mainly containing CO_2 (up to 10% in mass in some Italian geothermal reservoirs); however, it is frequent to find acid gases in the resource such as H_2S, a common contaminant in geothermal fields all over the world (Bates et al., 2015; Hartmann & Rydgren, 2018; Peralta et al., 2013). These, together with saline equilibria within the brine, can alter significantly the composition of the gas and liquid stream. The presence of acid gases is also a challenge for equipment, such as gas compressors and heat exchangers. For the purpose of the calculation of two-phase flow reinjection, it can be sufficient to apply proven models for the solubility of CO_2 in water (Duan

& Sun, 2003; O'Sullivan et al., 1985), usually are more accurate than methodologies widely applied in the Oil&Gas industry (often dealing with sour gas mixtures: hydrocarbons, CO_2 and H_2S). The original correlations for CO_2 solubility in water developed in (O'Sullivan et al., 1985)are also part of the software package TOUGH2 (Pruess et al., 1999) and are substantially replicated by the PHREEQC software (Parkhurst & Appelo, 1999) which are tools frequently used by experts in geochemistry (who must also deal with solid interaction, that is, rock porosity and salt precipitation). The model described in (Duan & Sun, 2003) was developed for applications in CCS, and has the advantage of including experimental validation at relatively high-temperatures (150-200°C), which are common in geothermal applications. One of the key issues is the dependence of the solubility of CO_2 in water on two variables, namely pressure and temperature, which is effectively represented in Figure 1, reporting a synthesis of the equilibrium correlation by (Duan & Sun, 2003). It can be seen that raising the pressure level allows increasing amounts of CO_2 to be dissolved in water, and that at pressure lower than 40 bar the temperature dependence of solubility is significant. In practice, this means that cooling the geothermal resource (extracting heat under pressurized conditions) maintains the NCGs dissolved within the liquid stream; moreover, this has a positive effect on scaling, because also precipitation of salts is reduced.

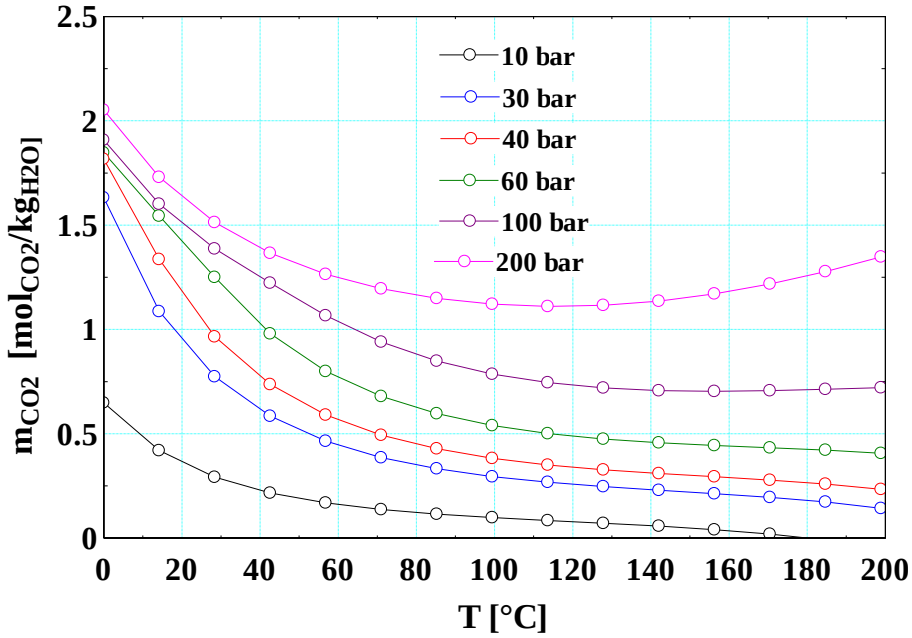

Figure 1: Solubility of CO_2 vs temperature at different pressures.

2.1 Application of the CO_2 solubility model

The solubility of CO_2 in the geothermal fluid is evaluated applying the model derived from (Duan & Sun, 2003). It is based on the theory of particle interactions for the liquid phase and on a proper equation of state for the vapour phase. The CO_2 solubility is obtained through the balance of the chemical potential of CO_2 in liquid and vapor phase ($\mu^l_{CO_2}$ and $\mu^v_{CO_2}$ respectively). The chemical potential can be expressed as a function of fugacity for the vapor phase (Equation 1) and activity for the liquid phase (Equation 2, (Pitzer, 1973)):

$$\mu^v_{CO_2}(T,p,y) = \mu^{v(0)}_{CO_2}(T) + RT\ln f_{CO_2}(T,p,y) = \mu^{v(0)}_{CO_2}(T) + RT\ln(y_{CO_2}p) + RT\ln\varphi_{CO_2}(T,p,y) \quad (1)$$

$$\mu^l_{CO_2}(T,p,m) = \mu^{l(0)}_{CO_2}(T,p) + RT\ln a_{CO_2}(T,p,m) = \mu^{l(0)}_{CO_2}(T,P) + RT\ln m_{CO_2} + RT\ln\gamma_{CO_2}(T,p,m) \quad (2)$$

The fugacity coefficient, φ, shows the deviation of a real gas from the ideal behaviour and the activity coefficient, γ, is the ratio of the actual fugacity of a solution to that at the standard state (Prausnitz et al., 1999). At equilibrium, $\mu^l_{CO2} = \mu^v_{CO2}$. Therefore, the CO_2 molality, m_{CO2}, can be calculated by the following relationship:

$$\ln\frac{y_{CO_2}P}{m_{CO_2}} = \frac{\mu^{l(0)}_{CO_2}(T,p) - \mu^{v(0)}_{CO_2}(T)}{RT} - \ln\varphi_{CO_2}(T,p,y) + \ln\gamma_{CO_2}(T,p,m) \quad (3)$$

In Equation 3, $\mu^{v\,(0)}_{CO2}$ can be set to zero, as the result of the current investigation is affected only by the difference between $\mu^{v\,(0)}_{CO2}$ and $\mu^{l\,(0)}_{CO2}$. Therefore, y_{CO2} is determined by:

$$y_{CO_2} = \frac{P - P_{H_2O}}{P} \quad (4)$$

p is the total pressure of the mixture ($p_{H2O} + p_{CO2}$). p_{H2O} is the saturation pressure of pure water at the mixture temperature, which is evaluated, in the present model, using the thermodynamic libraries or by an empiric correlation as in Duan and Sun, (2003).

The coefficient of activity γ is calculated by the following relationship:

$$\ln\gamma_{CO_2} = \sum_c 2\lambda_{CO_{2-c}} m_C + \sum_a 2\lambda_{CO_{2-a}} m_a + \sum_c \sum_a \zeta_{CO_{2-a-c}} m_C\, m_a \quad (5)$$

where λ and ζ are second-order and third-order interaction parameters, respectively; m_c and m_a are the molality of cations and anions, respectively. λ, ζ and $\mu_{CO2}^{l\,(0)}$ are determined by equation (6), which is a function of total pressure and temperature only:

$$f(\mathrm{T,p}) = c_1 + c_2 T + \frac{c_3}{T} + c_4 T^2 + \frac{c_5}{630-T} + c_6 p + c_7 p \ln T + c_8 \frac{P}{T} + c_9 \frac{P}{(630-T)} + c_{10} \frac{P^2}{(630-T)^2} + c_{11} T \ln p \qquad (6)$$

The c_i coefficients, which are different for λ, ζ and $\mu_{CO2}^{l\,(0)}$, are obtained from (Duan & Sun, 2003), while the fugacity of the vapor phase is directly computed by the internal libraries available in EES (Klein & Nellis, 2012).

3. TORRE ALFINA (IT) SITE, PROJECT SPECIFICATIONS, MODEL OF POWER PLANT AND VARIANTS

Torre Alfina geothermal site consists of a water-dominated reservoir with a pressure of about 44 bar, a temperature of 140°C (DGS-UNMIG, 2018b, 2018a), and with a relatively high share of NCGs. (about 2% by weight CO_2, 0.2% H_2S) (Buonasorte et al., 1988, 1991; Regione Umbria & Università di Perugia, 2013). The mining concession covers about 480 km^2 and it is in Central Italy between Latium, Tuscany and Umbria regions, close to Bolsena Lake, as shown in Figure 2. In this area, several production (5) and reinjection (4) wells are needed in order to exploit the geothermal resource and generate 5 MWe, which is the size of a pilot power for the Italian laws (DGS-UNMIG, 2019).

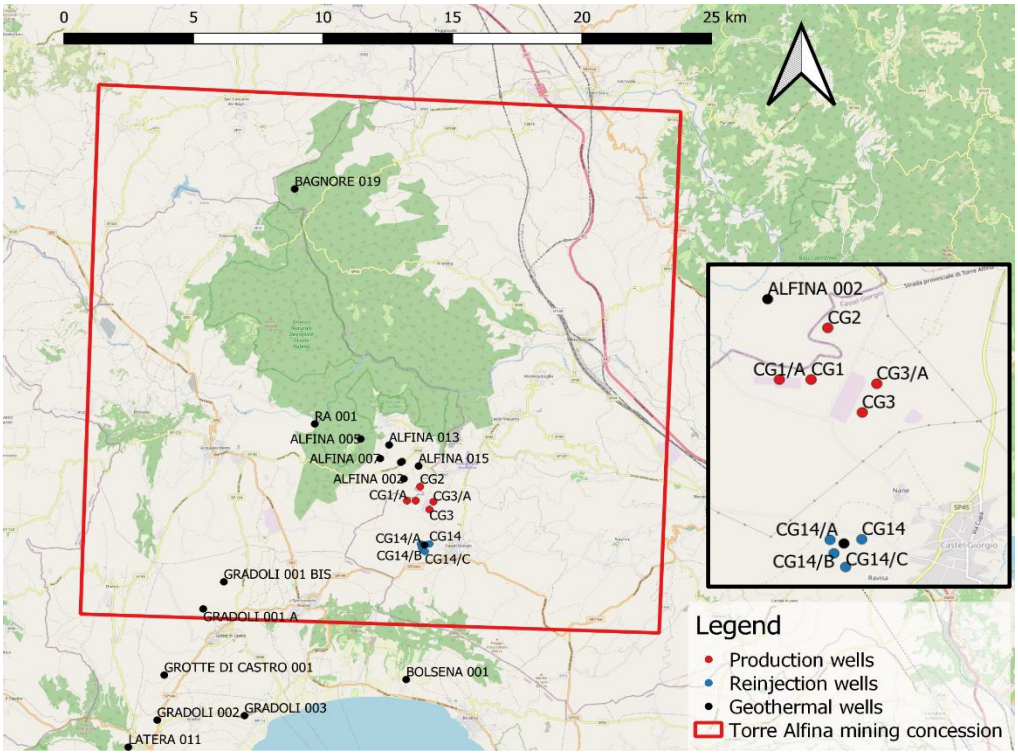

Figure 2: Torre Alfina mining concession and wells location.

Torre Alfina project details were obtained from the repository of the Italian Ministry of Environment and Protection of Land and Sea (Italian Ministry of the Environment and Protection of Land and Sea, 2018). The project considers a regenerative ORC cycle as the power plant for energy conversion, while comprises of a borehole pump for the closed-loop of geothermal fluid. The set reinjection temperature needed to be higher than 70°C due to scaling issues. The borehole pump pressurizes the geothermal fluid in order to have a well-head pressure of 44 bar, which is required in order not to let the NCGs form and stay soluble within the brine. Figure 1 displays a schematic of the power plant. The proposed scheme is flexible, as it allows to work both in the subcritical and supercritical region. Particularly, the original project foreseen the utilization of a subcritical isobutane cycle, however, due to the favourable working conditions (heat profile), a supercritical r1234yf solution is also assessed in this work.

The most critical components of the power plant are certainly the geothermal heat exchanger (HEgeo) and the borehole pump, as the expected size and operating pressure are not commonly achieved with aggressive geothermal fluid. Nonetheless, this solution guarantees the total reinjection of the geothermal fluid, avoiding the release of the NCGs and therefore improving the environmental footprint of the geothermal power plant.

Table 1: Main specifications and auxiliary data for the Torre Alfina power plant.

	Subcritical	**Supercritical**
T_{30} [°C]	140	140
P_{30} [bar]	44	44
$\dot{m}_{30}$ [kg/s]	313	218
CO_2 [w%]	2	2
Fluid	isobutane	R1234yf
P_6 [bar]	14.82	41.98
T_6[°C]	85	120

$\dot{m}_6$ [kg/s]	269	426
η_T, η_P [-]	0.87, 0.8	0.87, 0.8
ΔT_{PP} [°C]	5	5

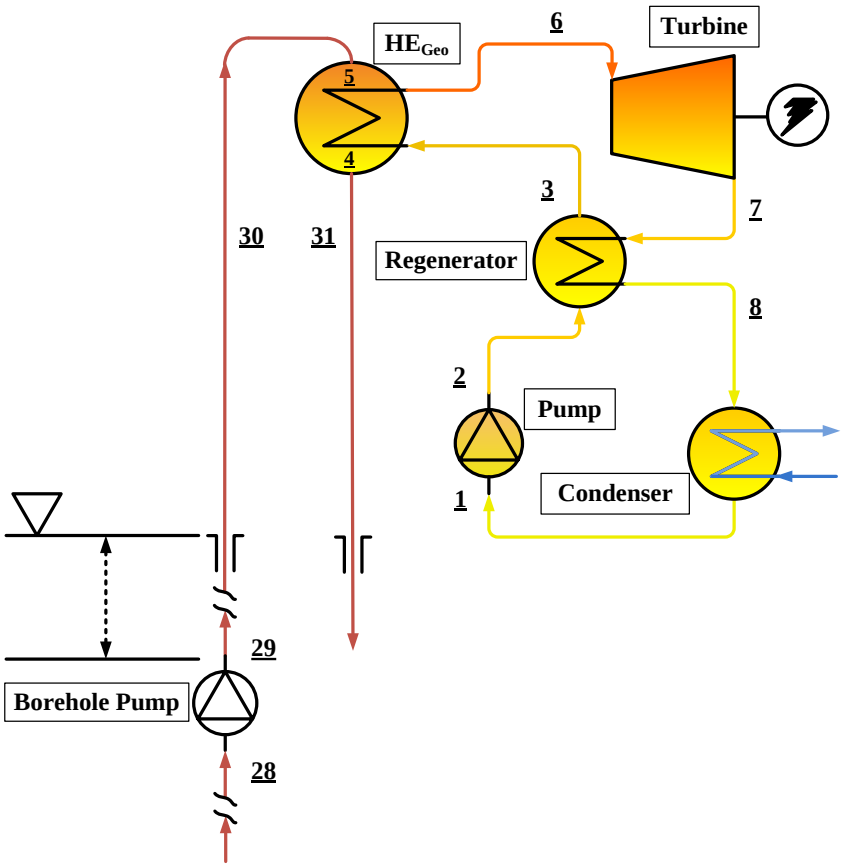

Figure 3: General layout of power plant (brine and ORC circuits).

4. ENERGY, EXERGY, EXERGO-ECONOMIC AND EXERGO-ENVIRONMENTAL ANALYSES

The thermodynamic performance calculations were carried out through the setting of mass, energy and exergy balances, as suggested in (Bejan et al., 1996). To compute the thermodynamic properties of the ORC working fluid, internal library routines of EES software were utilized (Klein & Nellis, 2012), while for the properties of the geothermal brine, specific libraries available in Unisim® or TREND 3.0 were used. The reference state for the exergy analysis was set at 25°C and 101.325 kPa. Exergy losses derived from the reinjection of the brine were not taken into account. Conversely, the exergy loss caused by the heat rejected to the environment by the cooling towers was included.

The Exergo-Economic Analysis (EEA) is based on the cost evaluation of the power plant equipment. The equipment costs were calculated by validated cost correlations, (Mwawasi, 2014; Turton, 2013) reported in Table 2; the set of Equations 8-10 was applied for scaling of the equipment costs. For the specific case of a binary geothermal plant, a relevant cost is represented by the production and reinjection wells; this cost was evaluated following accepted published correlations (Dumas et al., 2013) . The EEA defines a "fuel" and a "product" for each plant component, following the consolidated SPECO approach (Lazzaretto & Tsatsaronis, 2006). At this stage the exergy destruction is known for each component, and its cost can be calculated.

The cost of the wells was calculated as a capital cost needed for plant operation; dividing it by the operational lifetime, and by the exergy of the inlet brine and determined as the "fuel" cost at plant inlet (that is, ahead of the borehole pump).
The wells cost is at the origin of the plant inlet fuel cost, scaled by the total exergy input from the geothermal brine, as shown in Equation 7:

$$C_{fuel} = \frac{C_{wells}}{Ext_{in}} \tag{7}$$

Where C_{wells} is the cost of 5 productions wells and 4 reinjections wells and Ext_{in} is the total extracted exergy from the geothermal resource during the whole life of the power plant (here assumed at 20 years with 7446 hours of operation per year (Fiaschi et al., 2017)

Following accepted practice (Bejan et al., 1996) the cost of the loss (taking place at the condenser/cooling tower) is calculated and re-assigned to all streams proportionally to the flow of "fuel" exergy. The exergo-economic analysis allows the calculation of the

buildup of the unit cost of exergy along the plant (the final result is electricity, exergy equal to mechanical output power), so that the production cost of kWh can be calculated. The EEA also provides an insight about the possibilities of power plant improvement, by identifying the components responsible of the largest costs in terms of capital and exergy destruction.

Table 2: Equipment Cost Correlations

Component	**Cost correlantion [€]**	**Cost balance equations**	**Auxiliary equations**
BH Pump	1000*W_{BHp}	$c_{29}\dot{E}x_{29} = c_{28}\dot{E}x_{28} + c_{W_{BHp}}\dot{W}_{BHp} + \dot{Z}_{BHp}$	$c_{W_{BHp}}=c_{W_t}$ $c_{29} = c_{30}$
Pump	$C_P^0 * F_{BM}$	$c_2\dot{E}x_2 = c_1\dot{E}x_1 + c_{W_p}\dot{W}_p + \dot{Z}_p$	$c_{W_p}=c_{W_t}$
Regenerator	$C_P^0 * F_{BM}$	$c_3\dot{E}x_3 + c_8\dot{E}x_8=c_2\dot{E}x_2+c_7\dot{E}x_7+\dot{Z}_{HE}$	$c_7 = c_8$
HEgeo	$C_P^0 * F_{BM}$	$c_6\dot{E}x_6+c_{31}\dot{E}x_{31} + c_{40}\dot{E}x_{40} = c_3\dot{E}x_3+c_{30}\dot{E}x_{30}+\dot{Z}_{HEgeo}$	$c_{30} = c_{31}$ $c_{40} = c_{30}$
Turbine	$C_P^0 * F_{BM}$	$c_7\dot{E}x_7 + c_{W_t}\dot{W}_t = c_6\dot{E}x_6+\dot{Z}_t$	$c_6 = c_7$
Condenser	$C_P^0 * F_{BM}$	$c_1\dot{E}x_1 + c_{21}\dot{E}x_{21} = c_8\dot{E}x_8 + c_{20}\dot{E}x_{20} + \dot{Z}_{cond}$	c_{20}=0 $c_{21} = c_{20}$

$$C_{BM} = C_P^0 * F_{BM} \quad (8)$$

$$\log_{10} C_P^0 = K_1 + K_2\log_{10}(X) + K_3(\log_{10}(X))^2 \quad (9)$$

$$F_{BM} = (B_1 + B_2 F_P F_M) \quad (10)$$

Where W_{BHP} is the power of the borehole pump in [kW]; C_{BM} is the bare module cost, which includes the direct and indirect cost of the component; C_P^0 is the base cost of the component; F_{BM} is the bare module factor, which takes into account the cost correction as a function of operating pressure and material of the component; X is the functional unit of the component (the heat-transfer area for heat exchangers; the rated power for pump and turbine); K_1, K_2, K_3, B_1, B_2, F_P, F_M are correction coefficients that are tabled in (Turton *et al.*, 2013).

After the economic analysis, the environmental performance of the power plant is evaluated using methodology developed by the European Commission to evaluate the environmental impacts of products and organisations (European Commission, 2013) called the Product/ Organisation Environmental Footprint (PEF/OEF or generically EF).

The Life Cycle Inventory (LCI) was built using PEF secondary database, implemented in the OpenLCA software (Ciroth et al., 2019), that contains datasets from the Life Cycle Data Network nodes listed in Table 3.

Table 3: List of EF compliant nodes used for life cycle modeling (European Commission, 2019)

Data type	**Data provider**	**Node**
EF representative products	European commission	http://eplca.jrc.ec.europa.eu/EF-node/
Chemicals for Paint	CEPE Ecoinvent	http://lcdn-cepe.org/
Textiles	Cycleco	https://node.cycleco.eu/node/
Chemicals	Ecoinvent	http://ecoinvent.lca-data.com/
Feed	Fefac	http://lcdn.blonkconsultants.nl/Node/
Agrofood, "others"	Quantis	https://lcdn.quantis-software.com/PEF/
Glass recycling	RDC	http://soda.rdc.yp5.be/login.xhtml
Energy and transport, packaging, metals, end-of-life, incineration, plastics, electronics, cooling and freezing transports	Thinkstep	http://lcdn.thinkstep.com/Node/

In this study, the evaluation is made using methodological framework EF 2.0 developed during the EF Pilot Phase. The input and output flows are classified and characterized using the international reference life cycle data system (ILCD) midpoint method for 16 impact categories, that covers all relevant environmental issues related to the electricity production. PEF standard normalization and weighting factors were used to quantify the single score environmental impact of each component of the system. The *functional unit* was assumed as 1 MWh of electricity. The analysis is run as a cradle-to-gate LCA. Therefore, it includes the construction and the operational phases. In fact, it is known that construction (with specific reference to the wells drilling) represents a relevant phase of the Life Cycle Impact of a geothermal power plant (Asdrubali et al., 2015).

The Exergo-Environmental analysis (EEvA) applies the same workflow of the Exergo-Economic model, using the environmental costs of components through a component-level disaggregation of the LCI and calculating the buildup of the environmental cost along the power plant. Regarding the wells and machinery equipment, data about the specific material consumption used LCA process were collected from the environmental assessments provided by the (Italian Ministry of the Environment and Protection of Land and Sea, 2018) . The main formulas for exergoeconomic and exergoenvironmental analyses are presented in Table 4.

Table 4: Main relationships for exergoeconomic and exergoenvironmental analysis

Exergoeconomic analysis	Exergoenvironmental analysis
Exergy stream cost rate $\dot{C}_j = c_j \cdot \dot{E}x_j$	Exergoenvironmental stream impact rate $\dot{B}_j = b_j \cdot \dot{E}x_j$
Component cost balance $\sum \dot{B}_{j,k,in} + \dot{Z}_k = \sum \dot{B}_{j,k,out}$	Component environmental impact balance $\sum \dot{B}_{j,k,in} + \dot{Y}_k = \sum \dot{B}_{j,k,out}$
Component-related cost rate (Table 2)	Component-related environmental impact rate $\dot{Y}_k = \dot{Y}_{CO} + \dot{Y}_{OM} + \dot{Y}_{DI}$
Component exergoeconomic factor $f_k = \frac{\dot{Z}_k}{\dot{Z}_k + \dot{C}_{D,k}}$	Component exergoenvironmental factor $f_{d,k} = \frac{\dot{Y}_k}{\dot{B}_{D,k} + \dot{Y}_k}$

5. RESULTS - ENERGY AND EXERGY MODELING

The performance indicators obtained for the assessed case study are resumed in figure 4. The two considered ORC configurations, subcritical isobutane and supercritical r1234yf are compared. As the geothermal resource is in sub-cooled liquid state, the matching of the T-Q curves is better for the supercritical cycle ORC. This implies a higher efficiency of the cycle, as well as a lower employment of the geothermal heat, as testified by the nearly 30% lower value of $\dot{Q}_{GEO}$. The utilization of lower geothermal heat implies that a lower consumption of the geothermal resource, potentially enhancing its lifetime.

The exergy analysis provide a way to identify the most impacting components of the power plant. A pie chart has been utilized in figure 5 in order to at first glance the most inefficient component of the power plants. Particularly, it is evident ad first sight that the supercritical ORC cycle achieve a higher efficiency due to a drastic reduction of the HEgeo exergy destruction, from 23.7% to 11.3%.

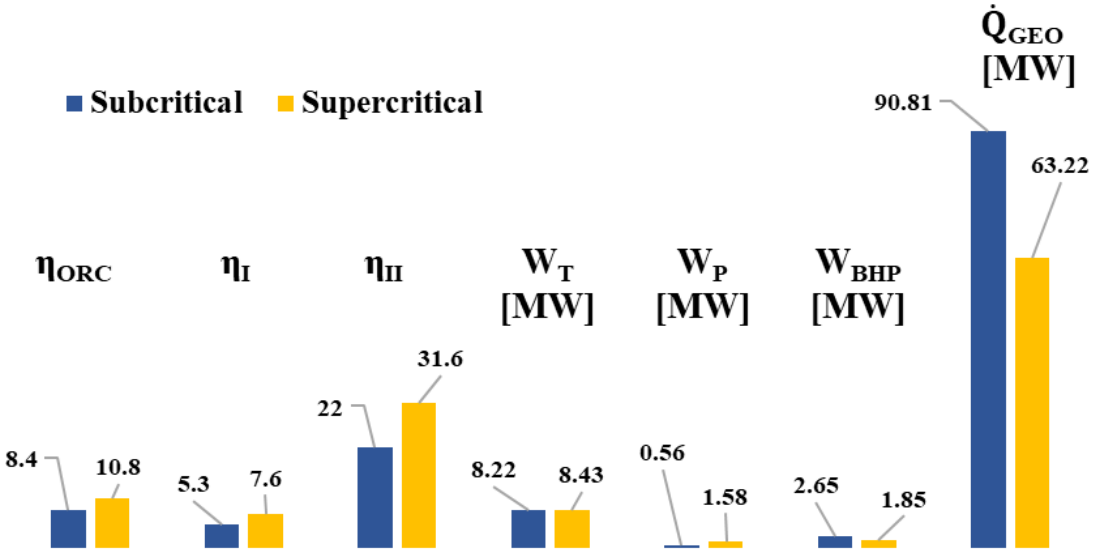

Figure 4: Performance parameters of ORC power plant.

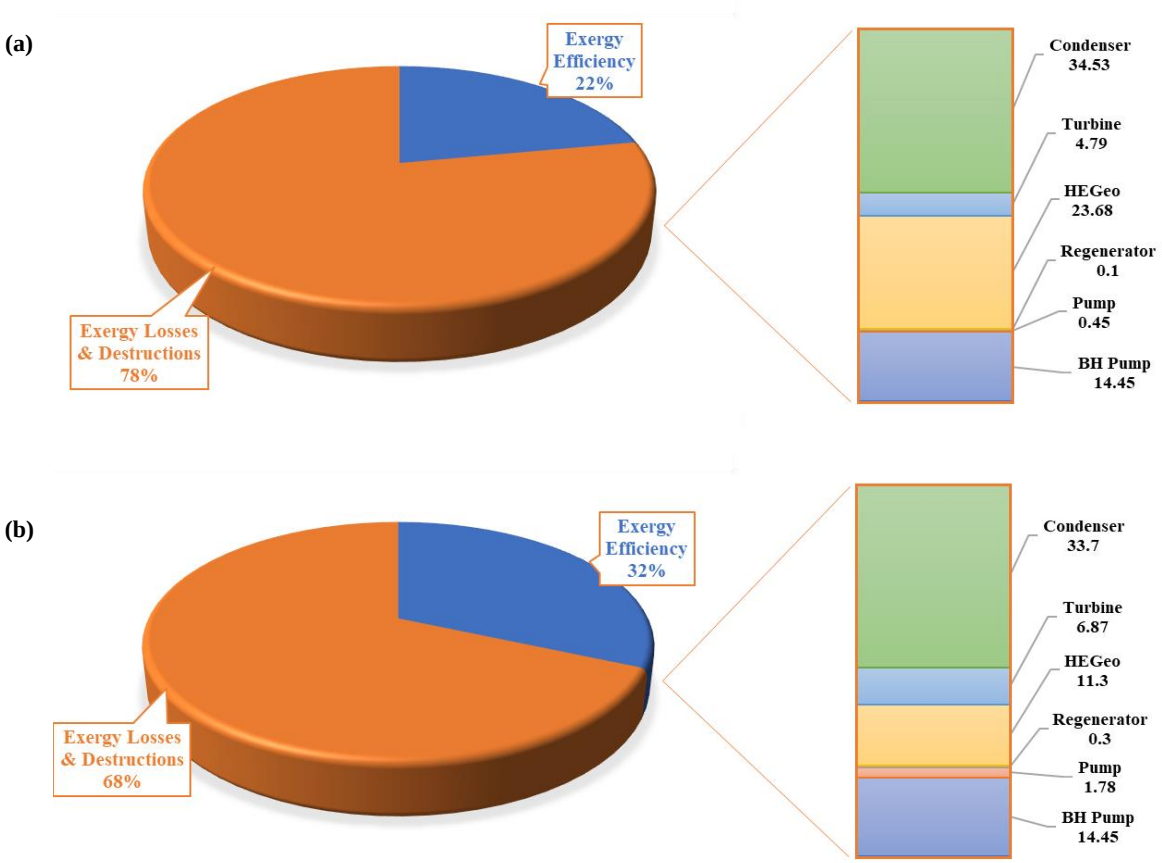

Figure 5: Second low efficiency and exergy destruction and losses of (a) subcritical and (b) supercritical cycles.

6. RESULTS: EXERGO-ECONOMIC AND EXERGO-ENVIRONMENTAL ANALYSES

Through the methodology explained in Section 5, it was possible to determine the specific investment cost of the system (excluding the cost of the wells) at 3790 €/kW for the subcritical cycle and 3383 €/kW for the supercritical cycle. These values are within the expected range, as stated in (International Renewable Energy, 2018). The results of the exergo-economic analysis are presented for the subcritical and the supercritical cycle in Tables 5 and 6.

The most expensive component of the power plant results, in both cases, the HE_{GEO}, which is indeed a challenging heat exchanger working at very high pressures with corrosive fluids (geothermal brine). Due to the low efficiency of the system (which is mainly attributable to the moderate temperature level of the resource), also the heat transfer surface of the condenser is large; as a consequence, also the investment cost of this component is relevant. Finally, in both cases cost of the BH pump is not negligible, resulting in the same range of the most cost-intensive components of the power plant. From the exergo – economic point of view, the most relevant component for both power plants is the condenser, due to its very high losses, followed by the turbine and the HE_{GEO}.

The output product cost for the turbine represents the levelized cost of electricity (LCOE), which is a fundamental outcome of the exergo-economic analysis. For the subcritical case, the LCOE is 13.33 c€/kWh, while for the supercritical cycle the LCOE is 13.11 c€/kWh. In the present case study, the total purchased equipment cost of the system (including BH pump) is 21.33 M€ for the subcritical cycle and 19.5 M€ for the supercritical cycle. The cost of wells drilling is 38 M€, which represents about 65% of the total plant costs for both cases.

As a consequence of the different use of the resource in the sub- and super-critical cases, the cost of the wells has a different impact on the inlet fuel cost, which is scaled by the total exergy input from the geothermal brine, as shown in Equation 7. However, the supercritical cycle is more efficient and this finally determines a small difference in the value of the LCOE. In both cases, as a consequence of the use of a liquid resource with high flow rates and a large number of wells (9) compared to the plant size (5 MWe), the value of the LCOE is relatively high (about double the value typical of plants operating on dry steam conditions or applying a flash for production of steam).

Table 5: Exergoeconomic results for the subcritical isobutane cycle.

Component	PEC (€)	$\dot{Z}_k$ (€/s)	$\dot{C}_{D,k}$ (€/s)	$\dot{Z}_k + \dot{C}_{D,k}$ (€/s)	$c_{F,k}$ (€/kWh)	$c_{P,k}$ (€/kWh)	f_k (−)
BH Pump	3.436E+06	0.02768	0.01026	0.03794	0.13338	0.190872	0.7295
Pump	347533	0.002799	0.00377	0.006569	0.13338	0.18468	0.4261
HE	1.137E+06	0.009161	0.0006835	0.009845	0.10926	0.204876	0.9306

HEgeo	5.552E+06	0.04472	0.03408	0.0788	0.0228096	0.03978	0.5675
Turbine	2.743E+06	0.0221	0.03294	0.05504	0.10926	0.13338	0.4015
Condenser	8.051E+06	0.06485	0.1329	0.1978	0.262656	0.38088	0.3279

Table 6: Exergoeconomic results for the supercritical R1234yf cycle.

Component	**PEC (€)**	$\dot{Z}_k$ (€/s)	$\dot{C}_{D,k}$ (€/s)	$\dot{Z}_k + \dot{C}_{D,k}$ (€/s)	$c_{F,k}$ (€/kWh)	$c_{P,k}$ (€/kWh)	f_k (−)
BH Pump	2.392E+06	0.01927	0.007027	0.0263	0.131184	0.188424	0.7328
Pump	1.252E+06	0.01008	0.01035	0.02043	0.131184	0.187848	0.4935
HE	2.233E+06	0.01799	0.00121	0.0192	0.107856	0.1989	0.937
HEgeo	6.570E+06	0.05292	0.01302	0.06593	0.026208	0.043668	0.8026
Turbine	2.747E+06	0.02212	0.03254	0.05466	0.107856	0.131184	0.4048
Condenser	4.281E+06	0.03448	0.14	0.1745	0.40428	0.558	0.1976

Figure 6 presents comparison of Environmental Footprint of high voltage electricity produced in the two analysed geothermal power cycles. It can be noticed that the EF single score for both cases is matching. For both cases, the highest contribution to the total impact value (83 and 82%, for sub and supercritical cycles, respectively) is due to the geothermal wells construction. Regarding the environmental impact of the working fluid, its contribution to the total impact is negligible; in absolute terms, isobutane is characterized by lower impact. Therefore, the working fluid contribution is smaller for the subcritical cycle, accounting for 0.2 % of the total impact. The share of the power cycle machinery is below 10%), with the turbine being the main contributor.

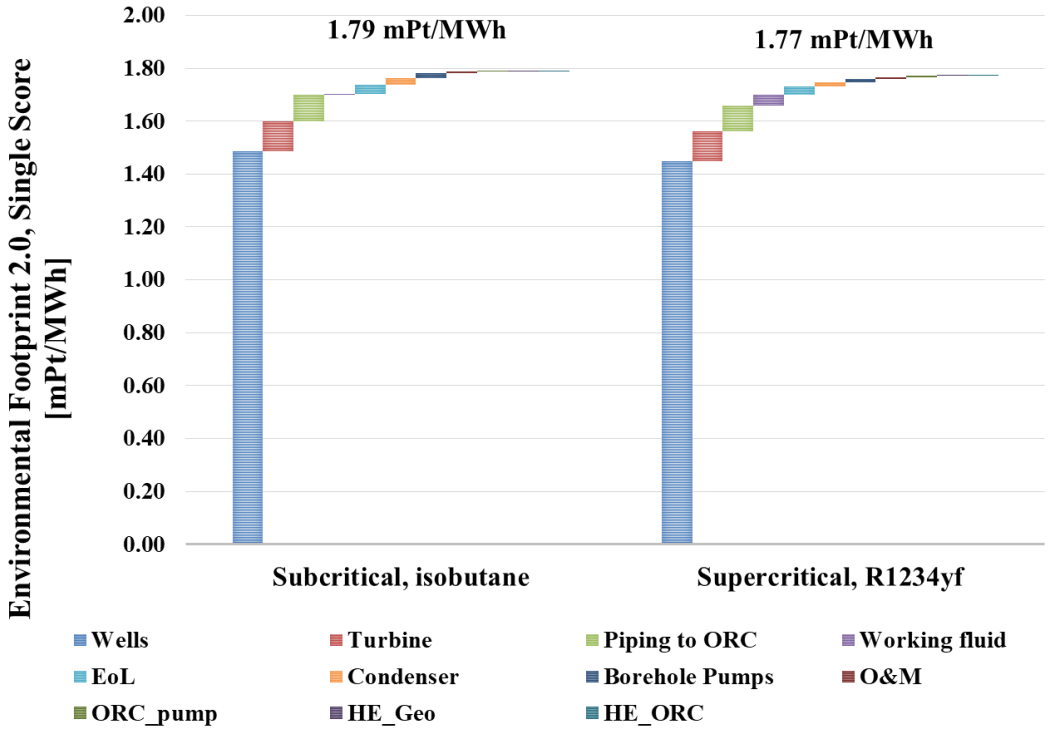

Figure 6: Comparison of EF2.0 Single Score environmental impacts of electricity produced in the geothermal plants

Figure 7 compares Environmental Footprint of high voltage electricity produced in the two analysed power cycles with those of other renewable energy systems. Previous literature studies comparing different electricity technologies, report the value of environmental impact of electricity produced with geothermal power plants in the range between wind and photovoltaic system for the most relevant LCA categories (Asdrubali et al., 2015). These studies were referred to powerplants without NCG sequestration. This study confirms that electricity from binary geothermal power plants have more favourable overall environmental performance compared to other renewable energy sources. As an example, the electricity produced in the binary geothermal power plant has around 10 times lower environmental impact than a biogas power plant. Only wind energy resulted in a lower single score EF impact. Tables 7 and 8 report results of the exergo – environmental analysis.

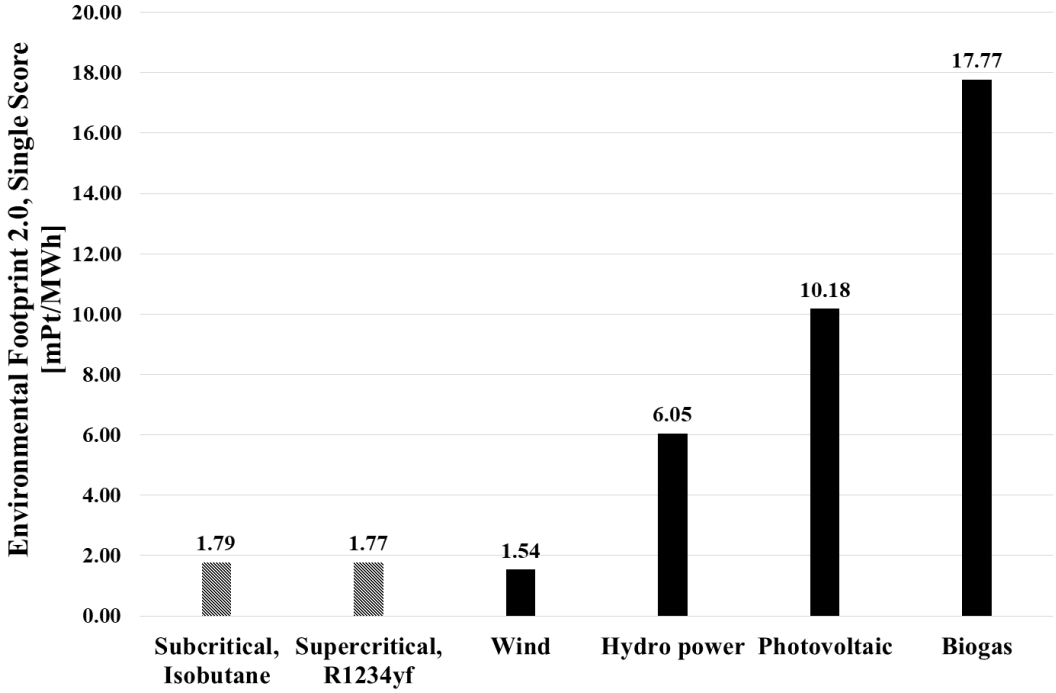

Figure 7: Comparison of Environmental Footprint 2.0 Single Score environmental impacts of electricity produced in the geothermal plants and other renewable – based power systems

Table 7: Exergoenvironmental results for the subcritical isobutane cycle.

Component	EF 2.0. Single Score (Pts)*	$\dot{Y}_k$ (mPts/h)	$\dot{B}_{D.k}$ (mPts/h)	$\dot{B}_{D.k} + \dot{Y}_k$ (mPts/h)	$f_{D.k}$ (%)	$r_{D.k}$ (%)
BH Pump	40.21	0.18	0.48	0.66	27.28	16.03
Pump	5.675	0.03	0.18	0.21	12.19	25.13
HE	1.398	0.01	0.03	0.04	15.81	7.28
HEgeo	119.2	0.53	2.51	3.05	17.5	33.46
Turbine	235.2	1.05	1.59	2.64	39.85	21.96
Condenser	94.08	0.42	6.33	6.75	6.239	32.27

*EF impacts of O&M and working fluid are attributed to the components on the basis of the their exergy destruction

Table 8: Exergoenvironmental results for the supercritical R1234yf cycle.

Component	EF 2.0. Single Score (Pts)*	$\dot{Y}_k$ (mPts/h)	$\dot{B}_{D.k}$ (mPts/h)	$\dot{B}_{D.k} + \dot{Y}_k$ (mPts/h)	$f_{D.k}$ (%)	$r_{D.k}$ (%)
BH Pump	34.6	0.15	0.39	0.55	28.26	16.25
Pump	25.37	0.11	0.58	0.69	16.4	26.16
HE	3.896	0.02	0.07	0.09	20.48	6.69
HEgeo	108	0.48	1.36	1.84	26.3	17.86
Turbine	276.9	1.24	1.82	3.06	40.51	21.66
Condenser	102.6	0.46	7.84	8.30	5.536	32.35

*EF impacts of O&M and working fluid are attributed to the components on the basis of the their exergy destruction

As can be observed, the component-related environmental impact $\dot{Y}_k$ of the turbine is the largest, followed by the main heat exchanger and condenser. The highest total exergoenvironmental impact at the component level ($\dot{B}_{D,k} + \dot{Y}_k$) is attributed to the condenser (6.75 mPts/h and 7.84 mPts/h, for the subcritical and supercritical power cycles, respectively) that contributes more than 50 % to the total exergoenvironmental impact of power plant machinery. Also, the turbine and the main heat exchanger present relevant (>10 %) scores ($\dot{B}_{D,k} + \dot{Y}_k$), in the range from 1.84 to 3.06 mPts/h. The higher the total environmental impact rate, the larger the influence of the component on the overall system; depending on the share of $\dot{Y}_k$ or $\dot{B}_{D,k}$, improvements of performance can be recommended for components having low $\dot{Y}_k$ and high $\dot{B}_{D,k}$ (Condenser, Turbine, HEgeo), while improvements regarding the design/materials economy can be recommended for components which has low $\dot{B}_{D,k}$ and a high $\dot{Y}_k$ (e.g. regenerative heat exchangers). Indeed, the condenser groups exergy destruction and exergy loss, with relevant flows of heat and exergy when compared to the reference state and stands thus as the component deserving the largest attention for the improvement of environmental performance.

7. CONCLUSIONS

A throughout assessment has been carried out in this manuscript, from the development of a thermodynamic analysis to detailed exergo-economic and environmental analyses. The performance results highlighted the higher efficiency of the supercritical ORC

cycle, which guarantees a reduced consumption of geothermal resource for a defined power production. The exergy analysis confirmed the obtained thermodynamic outcomes, pointing out the HE_{GEO} as the main contributor to the exergy destruction, while the condenser and the BH pump were the most critical components due to their exergy losses.

The exergo-economic analysis pointed out the crucial issue of large cost of the 5 production and 4 reinjection wells: this doubles the LCOE compared to the typical values of traditional dry-steam or flash geothermal power plants. Anyway, this LCOE may still be attractive in the light of the contributions allowed for power plants operating on such difficult resources. The condenser, the turbine and the borehole pump are identified as the power plant largest economic performance influencing components. – Anyhow, the cost of well drilling is definitely prevailing (it is about 65% of the overall geothermal project cost).

The LCA confirms that geothermal power plants with complete NCG reinjection are among the cleanest renewable energy technologies, with an edge even over wind energy. Again, the largest part of the environmental impact comes from the activity of well drilling in the construction phase, followed by the borehole pump; the surface powerplant equipment represents a minor share.

The exergo-environmental analysis confirms that the components deserving improvements in terms of environmental performance are the condenser, the turbine and the borehole pump; however, the improvement should focus in some cases on design/materials economy and in others on thermodynamic performance, depending on the relevance of $\dot{\boldsymbol{Y}}_{\boldsymbol{k}}$ or $\dot{\boldsymbol{B}}_{\boldsymbol{D,k}}$.

NOMENCLATURE

Symbols and acronyms

$\dot{B}$	Exergoenvironmental impact factor, mPts/s
$\dot{C}$	Exergy cost rate, €/s
$\dot{m}$	Mass flow rate, kg/s
$\dot{Q}$	Heat rate, kW
$\dot{W}$	Power, kW
$\dot{Y}$	Environmental impact factor, mPts/s
$\dot{Z}$	Instantaneous capital costs, €/s
BH	Borehole
c	Cost, €/kWh
EEvA	Exergo-environmental analysis
Ext	Exergy, kW
f	Exergoeconomic factor, (-)
HE	Heat exchanger
LCI	Life cycle inventory
LCOE	Levelized cost of energy
P	Pressure, bar
T	Temperature, °C
X	Functional unit
y	Molar fraction

Greek letters

ΔT	Temperature difference, °C
η	Efficiency
ζ	Third-order interaction parameters
μ	Chemical potential
φ	Fugacity coefficient, Pa
γ	Activity coefficient
η	Efficiency
λ	Second-order interaction parameter

Subscripts

0	Reference state

1,2,..	State point
BM	Bare module
D	Destruction
GEO	Geothermal brine
I	First law
II	Second law
j	Stream
k	Component
ORC	Organic Rankine Cycle
P	Pump
Pp	Pinch Point
T	Turbine

REFERENCES

Asdrubali, F., Baldinelli, G., D'Alessandro, F. & Scrucca, F. (2015). Life cycle assessment of electricity production from renewable energies: Review and results harmonization. *Renewable and Sustainable Energy Reviews*, *42*, 1113–1122. https://doi.org/10.1016/J.RSER.2014.10.082

Baldacci, A., Mannari, M. & Sansone, F. (2005). Greening of Geothermal Power : An Innovative Technology for Abatement of Hydrogen Sulphide and Mercury Emission. *World Geothermal Congress 2005*, *April*.

Bates, M. N., Crane, J., Balmes, J. R. & Garrett, N. (2015). *Investigation of Hydrogen Sulfide Exposure and Lung Function , Asthma and Chronic Obstructive Pulmonary Disease in a Geothermal Area of New Zealand*. 1–16. https://doi.org/10.1371/journal.pone.0122062

Bejan, A., Tsatsaronis, G. & Moran, M. J. (1996). *Thermal Design and Optimization*. John Wiley & Sons. https://doi.org/10.1016/S0140-7007(97)87632-3

Bruscoli, L., Fiaschi, D., Manfrida, G. & Tempesti, D. (2015). Improving the environmental sustainability of flash geothermal power plants-A case study. *Sustainability*, *7*(11), 15262–15283. https://doi.org/10.3390/su71115262

Buonasorte, G., Cataldi, R., Ceccarelli, A., Costantini, A., D'Offizi, S. & Lazzarotto, A. (1988). Ricerca ed esplorazione nell'area geotermica di Torre Alfina (Lazio-Umbria). *Boll.Soc.Geol.It.*, 265–337.

Buonasorte, G., Pandeli, E. & Fiordelisi, A. (1991). The Alfina 15 well: deep geological data from Northern Latium (Torre Alfina geothermal area). *Boll.Soc.Geol.It.*, 823–831.

Ciroth, A., Di Noi, C., Lohse, T. & Srocka, M. (2019). *OpenLCA 1.10, Comprehensive User Manual, GreenDelta GmbH, Berlin*. https://doi.org/10.1111/fcre.12450

DGS-UNMIG, M. dello sviluppo economico. (2018a). *Inventario delle risorse geotermiche nazionali*. http://unmig.sviluppoeconomico.gov.it/unmig/geotermia/inventario/inventario.asp (accessed 12.25.18).

DGS-UNMIG, M. dello sviluppo economico. (2018b). *Pozzi geotermici*. http://unmig.mise.gov.it/unmig/geotermia/pozzi/pozzi.asp (accessed 12.25.18).

DGS-UNMIG, M. dello sviluppo economico. (2019). *Ricerca di risorse geotermiche finalizzata alla sperimentazione di Impianti Pilota*. https://unmig.mise.gov.it/index.php/it/dati/risorse-geotermiche/ricerca-di-risorse-geotermiche-finalizzata-alla-sperimentazione-di-impianti-pilota (accessed 5.9.19).

Duan, Z. & Sun, R. (2003). An improved model calculating CO 2 solubility in pure water and aqueous NaCl solutions from 273 to 533 K and from 0 to 2000 bar. *Chemical Geology*. https://doi.org/10.1016/S0009-2541(02)00263-2

Dumas, P., Antics, M. & Ungemach, P. (2013). *Report on geothermal drilling*. http://www.geoelec.eu/wp-content/uploads/2011/09/D-3.3-GEOELEC-report-on-drilling.pdf (accessed on 12/07/2019).

Eberle, A., Heath, G., Nicholson, S., Carpenter, A., Eberle, A., Heath, G., Nicholson, S. & Carpenter, A. (2017). *Systematic Review of Life Cycle Greenhouse Gas Emissions from Geothermal Electricity Systematic Review of Life Cycle Greenhouse Gas Emissions from Geothermal Electricity*. *September*.

European Commission. (2013). Recommendation 2013/179/EU on the use of common methods to measure and communicate the life cycle environmental performance of products and organisations. *Official Journal of European Union, L 124*, 210. https://doi.org/doi:10.3000/19770677.L_2013.124.eng

European Commission. (2019). *European Platform on Life Cycle Assessment Nodes: approved or waiting for approval*. https://eplca.jrc.ec.europa.eu/LCDN/contactListEF.xhtml (accessed 1.12.2020)

Fiaschi, D., Manfrida, G., Rogai, E. & Talluri, L. (2017). Exergoeconomic analysis and comparison between ORC and Kalina cycles to exploit low and medium-high temperature heat from two different geothermal sites. *Energy Conversion and Management*, *154*(November), 503–516. https://doi.org/10.1016/j.enconman.2017.11.034

Guo, B., Li, G., Song, J. & Li, J. (2017). A feasibility study of gas-lift drilling in unconventional tight oil and gas reservoirs. *Journal of Natural Gas Science and Engineering*. https://doi.org/10.1016/j.jngse.2016.11.057

Hartmann, J. & Rydgren, B. (2018). *Geothermal Sustainability Assessment Protocol Hellisheidi Geothermal Project GSAP*.

International Renewable Energy. (2018). Renewable power generation costs in 2018. In *International Renewable Energy Agency*.

Italian Ministry of the Environment and Protection of Land and Sea. (2018). *Impianto pilota geotermico denominato "Torre Alfina", Acquapendente (VT) - VAS - VIA - AIA.*

Kagel, A., Bates, D. & Gawell, K. (2005). *A guide to geothermal energy and the environment*. Geothermal Energy Association, Washington, DC (USA). https://doi.org/10.2172/897425

Klein, S. & Nellis, G. (2012). *Mastering EES, f-Chart software*.

Lazzaretto, A. & Tsatsaronis, G. (2006). SPECO: A systematic and general methodology for calculating efficiencies and costs in thermal systems. *Energy*. https://doi.org/10.1016/j.energy.2005.03.011

Mwawasi, H. M. (2014). *Feasibility study of using a downhole pumping system in Menengai well MW -17 for geothermal utilization.*

O'Sullivan, M. J., Bodvarsson, G. S., Pruess, K. & Blakeley, M. R. (1985). Fluid and Heat Flow In Gas-Rich Geothermal Reservoirs. *Society of Petroleum Engineers Journal*, *25*(2), 215–226. https://doi.org/10.2118/12102-PA

Parkhurst, D. L. & Appelo, C. A. J. (1999). *USER'S GUIDE TO PHREEQC (VERSION 2)— A COMPUTER PROGRAM FOR SPECIATION, BATCH-REACTION, ONE-DIMENSIONAL TRANSPORT, AND INVERSE GEOCHEMICAL CALCULATIONS* (Issue Version 2).

Peralta, O., Castro, T., Durón, M., Salcido, A., Celada-murillo, A., Navarro-gonzález, R., Márquez, C., García, J., De, J., Torres, R., Villegas-martínez, R., Carreón-sierra, S., Imaz, M., Martínez-arroyo, A., Saavedra, I., De, M., Espinosa, L. & Torres-jaramillo, A. (2013). Geothermics H 2 S emissions from Cerro Prieto geothermal power plant , Mexico , and air pollutants measurements in the area. *Geothermics*, *46*, 55–65. https://doi.org/10.1016/j.geothermics.2012.12.001

Pitzer, K. S. (1973). Thermodynamics of electrolytes. I. Theoretical basis and general equations. *Journal of Physical Chemistry*. https://doi.org/10.1021/j100621a026

Prausnitz, J. M., Lichtenthaler, R. N. & de Azevedo, E. G. (1999). Molecular Thermodynamics of Fluid-Phase Equilibria. In *Journal of Chemical Information and Modeling*.

Pruess, K., Oldenburg, C. M. & Moridis, G. J. (1999). *TOUGH2 User ' s Guide Version 2*.

Regione Umbria & Università di Perugia. (2013). *Studio delle potenzialità geotermiche del territorio regionale umbro Report finale*.

Rice, K. M., Walker, E. M., Wu, M., Gillette, C. & Blough, E. R. (2014). Environmental mercury and its toxic effects. In *Journal of Preventive Medicine and Public Health*. https://doi.org/10.3961/jpmph.2014.47.2.74

Shafaei, M. J., Abedi, J., Hassanzadeh, H. & Chen, Z. (2012). Reverse gas-lift technology for CO2 storage into deep saline aquifers. *Energy*. https://doi.org/10.1016/j.energy.2012.07.007

Snæbjörnsdóttir, S., Oelkers, E. H., Mesfin, K., Aradóttir, E. S., Dideriksen, K., Gunnarsson, I., Gunnlaugsson, E., Matter, J. M., Stute, M. & Gislason, S. R. (2017). The chemistry and saturation states of subsurface fluids during the in situ mineralisation of CO2 and H2S at the CarbFix site in SW-Iceland. *International Journal of Greenhouse Gas Control*. https://doi.org/10.1016/j.ijggc.2017.01.007

Turton, R. (2013). Analysis, Synthesis, and Design of Chemical Processes Fourth Edition. In *Journal of Chemical Information and Modeling*.